

Experimental Evaluation of Robustness of Panel-Method-Based Path Planning for Urban Air Mobility

Zeynep Bilgin, Murat Bronz, Ilkay Yavrucuk

▶ **To cite this version:**

Zeynep Bilgin, Murat Bronz, Ilkay Yavrucuk. Experimental Evaluation of Robustness of Panel-Method-Based Path Planning for Urban Air Mobility. AIAA AVIATION 2022 Forum, Jun 2022, Chicago, France. 10.2514/6.2022-3509 . hal-03948330

HAL Id: hal-03948330

https://enac.hal.science/hal-03948330

Submitted on 20 Jan 2023

HAL is a multi-disciplinary open access archive for the deposit and dissemination of scientific research documents, whether they are published or not. The documents may come from teaching and research institutions in France or abroad, or from public or private research centers.

L'archive ouverte pluridisciplinaire **HAL**, est destinée au dépôt et à la diffusion de documents scientifiques de niveau recherche, publiés ou non, émanant des établissements d'enseignement et de recherche français ou étrangers, des laboratoires publics ou privés.

Experimental Evaluation of Robustness of Panel-Method-Based Path Planning for Urban Air Mobility

Zeynep Bilgin*
Middle East Technical University, Ankara, 06800, Turkey

Murat Bronz†
ENAC, École Nationale de l'Aviation Civile, Université de Toulouse, Toulouse, France

Ilkay Yavrucuk‡
Middle East Technical University, Ankara, 06800, Turkey

In this study, robustness of panel method based path planning algorithm under wind disturbances is evaluated experimentally. Panel method, borrowed from fluid dynamics domain, is a numeric tool for calculating the potential field around arbitrarily shaped objects. Resultant potential field can be used for generating collision free trajectories for uncrewed aerial vehicles with convergence guarantee. Robustness of the proposed method is demonstrated during indoor experiments with a wind generator creating wind speed up to 7 m/s and also during outdoor experiments with wind speeds ranging between 3 - 5 m/s. Experiment results suggest that panel method based path planning scheme maintains its obstacle avoidance property under wind disturbances.

I. Nomenclature

K	=	Coefficient matrix
x, y, or d	=	Distance
q	=	Flow velocity induced by a vortex
u and v	=	Flow velocity components
N	=	Number of vehicles
β	=	Panel orientation angle
s	=	Panel length
Γ or γ	=	Vortex strength
Subscript	=	**Meaning**
∞	=	Free stream
i and j	=	Panel number
$sink$	=	Sink element
$source$	=	Source element

II. Introduction

VERTICAL Take-off and Landing (VTOL) vehicles offer a promising solution to ground traffic congestion in densely populated cities. Utilizing low-emission aircraft for the transport of people and goods over short distances could make a contribution to mobility in the future and reduce mobility-related emissions. Research institutions,established companies and start-ups are working on possible configurations of such aircraft and are examining the integration into the existing mobility system and the market potential of air mobility transport solutions. [1–4]. Having fully autonomous vehicles that can generate collision free paths not only increases the capacity of the urban air space but also reduces the urban air traffic management efforts [5]. Therefore, path planning in urban environments is an important issue to be addressed. Moreover,

*PhD Candidate, Aerospace Engineering Department, e188254@metu.edu.tr, AIAA Student Member.
†Assistant Professor, ENAC-Lab, Dynamic Systems, murat.bronz@enac.fr, AIAA Member.
‡Associate Professor, Aerospace Engineering Department, yavrucuk@metu.edu.tr, AIAA Member.

evaluation of path planning algorithms in realistic experimental settings with disturbances is crucial to asses effectiveness.

Classical approaches to path planning for autonomous vehicles can be divided into two sub categories: optimization problem based methods and potential field based methods. The first approach is formulating the problem as a large optimization problem with constraints [6–9]. Second approach is using artificial potential fields to generate collision free paths [7, 10–13]. Main advantage of this approach is its simplicity and easy implementation. The potential field method suffers from two major drawbacks. First one, the vehicle may get trapped in a local minima and secondly, the vehicle cannot reach to its destination if there are obstacles nearby due their repulsive force [14, 15]. Harmonic potential fields, a sub category of potential field based approaches, overcome the local minima limitation and produce constrained and well-behaved robot trajectory in static and dynamic environments [16–20]. One specific harmonic potential field that can be used in path planning is potential field of an irrotational flow of an ideal fluid [13, 21]. Panel method is a numerical tool that calculates the potential field of the fluid flow around arbitrarily shaped objects. This method is previously used for robot motion planning in literature [22–24]. Recently, panel method solution is used for addressing path planning problem in urban air mobility [25, 26] where assuming complete knowledge of the city map, path of each vehicle in an air taxi fleet is determined simultaneously using panel method.

In this paper the method proposed in [25, 26] previously developed at Middle East Technical University (METU) is tested in a realistic simulation environment and hardware experiments are conducted with Ecole Nationale de l'Aviation Civile (ENAC) in France through an international collaboration effort. Aim of this study is to test the robustness of the algorithm under the effects of wind gusts. Hardware experiments are conducted for both indoor and outdoor scenarios. Indoor flights took place in The Toulouse Occitanie Drone Flight Arena located in France. The flight area that is equipped with high-precision localisation and measuring instruments is one of the most hi-tech instrument equipped indoor flight zones in Europe[27]. Wind gusts in indoor arena are generated with a wind modular wind generator. Outdoor experiments are held in a local RC airfield runway located in Muret, France.

Main contributions of this study are as follows:

- Addition of a correction term during velocity calculation step in order to improve disturbance rejection performance of panel method based path planning algorithm.
- Field testing and verification of the robustness of panel method based path planning algorithm, both in an indoor flight arena with wind disturbance as well as in outdoor flights with real wind.

III. Methodology

Panel method based path planning algorithm was presented in previous studies[25, 26].

A. Panel Method Preliminaries

Panel method is a numerical tool for approximating potential field generated by the irrotational flow of an ideal fluid around arbitrarily shaped objects. To utilize panel method, the surfaces of the obstacles are divided into discrete elements called panels and a flow element (i.e. vortex, doublet, source etc.) is prescribed on each panel (Figure 1). In this study, prescribed flow elements are point vortices. Velocity induced by each panel on other panels can be calculated in terms of unknown vorticity strength γ. Then, unknown vorticity strengths can be found by setting the normal component of velocity on the obstacle surface to zero. After applying this boundary condition, panel method problem can be expressed as system of linear equations given in Eq. (1).

$$K_{ij}\gamma_j = RHS_i \tag{1}$$

$$K_{ij} = (u, v)_{ij} \cdot \vec{n}_i \tag{2}$$

$$\begin{bmatrix} u \\ v \end{bmatrix} = \frac{\gamma_j}{2\pi r_j^2} \begin{bmatrix} 0 & 1 \\ -1 & 0 \end{bmatrix} \begin{bmatrix} x - x_i \\ y - y_i \end{bmatrix} \tag{3}$$

Here, K_{ij} is a coefficient matrix and γ_j are the unknown vortex strengths. Components of K_{ij} are normal velocity induced by jth panel on ith panel.

$$RHS_i = -u_\infty \cos\beta_i - v_\infty \sin\beta_i \tag{4}$$

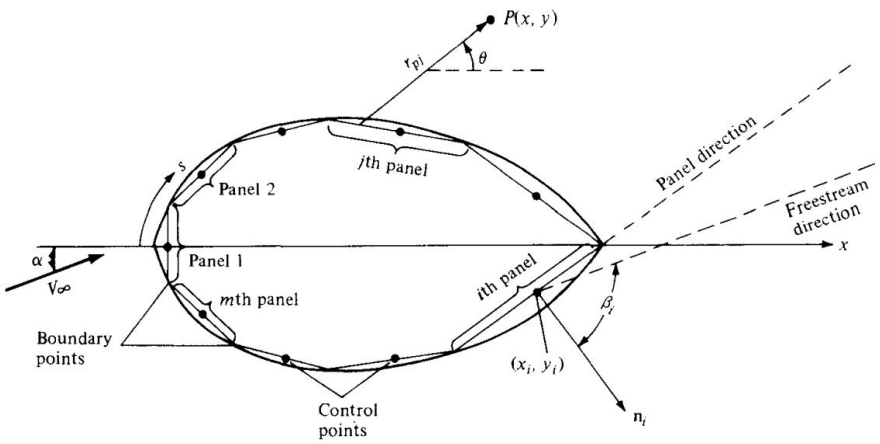


Fig. 1 Panel distribution over the surface of a body of arbitrary shape. [28]

The matrix RHS_i is obtained using free stream velocity components. Solving the system of linear equations given in Eq. (1) vortex strength on obstacle surfaces are obtained. After the strength of every flow element on the map is known, the fluid velocity at any point can be calculated and fluid streamlines can be obtained. Resultant streamlines can be used as vehicle trajectories in path planning problem.

Panel method is well studied in fluid mechanics and aerodynamics domain. Reader may refer to [28, 29] for detailed derivation of panel method.

B. Panel Method in Path Planning Problem

Following [25, 26]; resultant streamlines can be used as vehicle trajectories in path planning problem.

By definition fluid streamlines avoid collision with objects on their path. Hence, panel method has built in obstacle avoidance property. Collisions between vehicles can be avoided by modelling each vehicle as a point source element as in Eq. (5).

$$\begin{aligned} RHS_i = &- u_\infty \cos\beta_i - v_\infty \sin\beta_i - \sum_{n=1}^{N_{eVTOL}} u^n_{source} \cos\beta_i - \sum_{n=1}^{N_{eVTOL}} v^n_{source} \sin\beta_i \\ &- u_{sink} \cos\beta_i - v_{sink} \sin\beta_i - u_{safety} \cos\beta_i - v_{safety} \sin\beta_i \end{aligned} \tag{5}$$

Here, u_∞ and v_∞ are components of free stream velocity. N is the total number of vehicles. u_{source} and v_{source} are velocities induced by point source elements. The goal position is represented as a point sink element and velocity induced by sink element is prescribed as u_{sink} and v_{sink} in Eq. (5). u_{safety} and v_{safety} elements are the velocities induced by *safety source element* introduced in [26]. Safety source element is an point source element that travels with the vehicle itself. The safety source element amplifies the vortex strengths on the obstacle edges that are in the vicinity of the vehicle. Consequently, obstacles push the vehicle further away to a safer distance.

After all the unknown vortex strengths are found, flow velocity at any point can be calculated. Calculated flow velocity is fed to the vehicles as velocity command. In order to reduce deviation from original path under disturbance, a correction term is introduced and fed back to the velocity calculation with velocity error and its derivative using a PD controller.

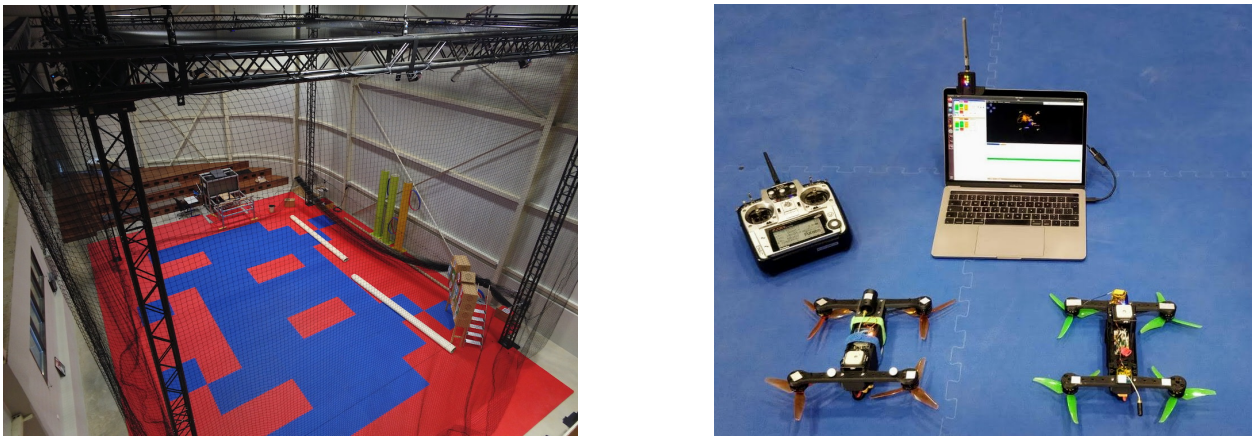
Reader may refer to [25, 26] for detailed derivation of method.

IV. Experimental Setup

One of the main contributions of this study is the experimental demonstration of the proposed method and verification of its robustness to unknown wind disturbance. For both indoor and outdoor experiments, ENAC's existing infrastructure for autonomous systems is utilized. This section briefly explains the autopilot system, indoor and outdoor flight setup, and wind generation method.

A. Indoor Flight Facility

The indoor experimental facility at ENAC consists of a 8 m $\times$ 8 m $\times$ 8 m flight volume with a mesh exterior, as shown in Fig. 2a. Obstacles with various shapes and heights are inserted into the 8m×8m×8m flight area to model a scaled urban environment. A 16-camera Optitrack system is used to track the motion of the quadrotors with sub-millimetre resolution in real time—a feature that is replaced by considerably less accurate GPS when flying outdoors. The quadrotors are called Explorer 1 and Explorer 2, and are shown in Fig. 2b. Including the battery, their mass is 535 g and their maximum thrust is 40 N. A 3-cell battery operates at 11.1 V and contains 2,300 mAh, which provides roughly 15 minutes of flight time.



(a) Indoor flight arena. **(b) Ground control station and quadrotors.**

Fig. 2 Indoor flight facility of ENAC.

B. WindShape - The Wind Generator

To test the robustness of the algorithm under effects of unknown wind gusts, the wind generator shown in Fig. 3 is used. *WindShape* is a modular wind generator located inside ENAC's indoor flight facility. Spatial wind control is

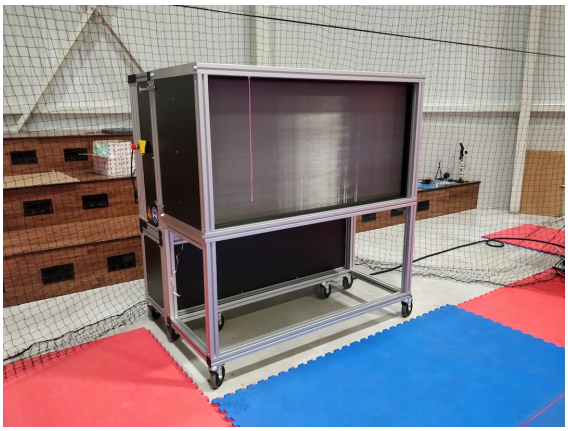


Fig. 3 WindShape, wind generator located inside ENAC's indoor flight facility.

possible via *wind pixels*, which are individual counter-rotating small electric fans. These fans have very low moment of inertia compared to traditional wind tunnel fans, making them easier to change the rotation rate, hence rapid variation of the wind speed. However during the presented experiments, the spatial wind speed have been kept constant.

C. Outdoor Flight Facility

Outdoor runway experiments are conducted in a local RC airfield runway located in Muret, France, that is 124 m $\times$ 12.5 m in size, as shown in Fig. 4a. ENAC has privileged access to this airfield, and can do tests in a volume of 500 m radius and up to 150 m height (which can be increased to 450 m in certain cases). Different quadrotors were used for the outdoor flights. They consist of the same avionics and propulsion system used on the indoor quadrotors, but are additionally equipped with Ublox-M8 GPS receiver which supplies 5 Hz position information with an accuracy of approximately 1.5 m. The quadrotors that are used for the outdoor flights are shown in Fig. 4b alongside with the ground control station (ordinary laptop), safety-pilot transmitters, and an XBee radio-modem that is used for telemetry and down-link communication.



(a) Outdoor flight field.



(b) Ground control station and outdoor quadrotors.

Fig. 4 Outdoor flight facility of ENAC, in Muret, Toulouse.

D. Paparazzi Autopilot System

Throughout the whole flight tests, we have used the Paparazzi Autopilot system [30]. It is an open-sourced project started back in 2003 and used by several research groups, academics, and hobbyists. Being one of the first open-source autopilot systems in the world, *Paparazzi* covers all three segments: ground, airborne, and the communication link between them. *Paparazzi* has also its complete flight plan language, where the user can define any possible trajectory using existing commands, such as circle, line, hippodrome, figure-eight, survey, etc. Additionally, any function written in C language can be called from the flight plan and executed. This opens up a lot of application possibilities, such as triggering a navigation procedure via a sensor output. Its integrated ground control station permits to control the flight plan execution, to move waypoints, or change any parameters of the aircraft while in flight.

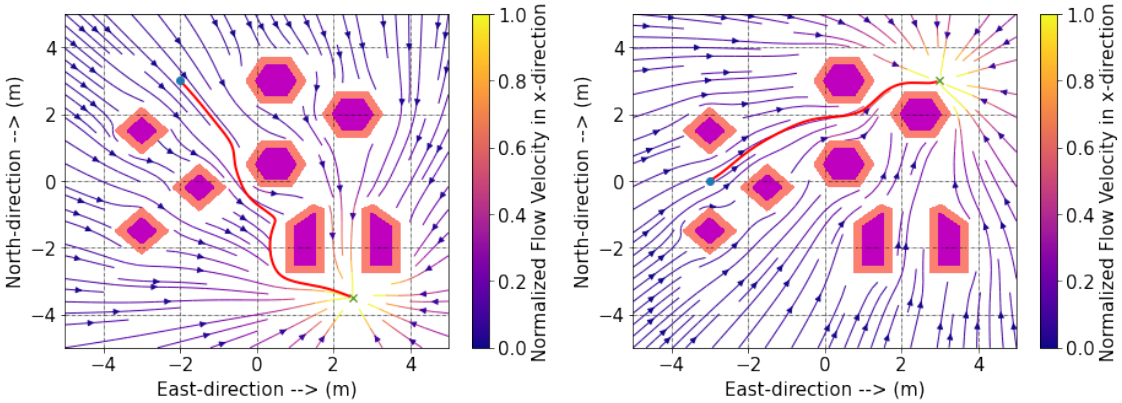
During both indoor and outdoor flights, the position of the vehicles are known (indoor:OptiTrack, outdoor: GPS plus on-board estimation), and therefore the calculated flow-field velocity for each vehicle serves as a reference velocity to follow. This reference is being updated at a frequency of 10Hz during the flights and once the velocity error between the reference and actual velocity is calculated, it is directly used as an input to the guidance control algorithm. Quadrotors use an Incremental Nonlinear Dynamic Inversion (INDI) [31] based guidance outer-loop to calculate the reference attitude and rotation rate, and later a cascaded INDI inner-loop calculates the required motor rpm increments.

V. Results

A. Simulation Results

During development, performance of the proposed path planning algorithm is tested on a simulation environment. Simulation results for two sample scenarios are plotted in Fig.5. In this figure, geometric shapes in magenta represent the cross-sections of various buildings in an scaled urban environment. Although panel method can provide a potential field

around any arbitrarily shaped obstacle; square, hexagon and trapezoid obstacles are selected for ease of manufacture in hardware experiments.



(a) Streamlines and path of vehicle 1. **(b) Streamlines and path of vehicle 2.**

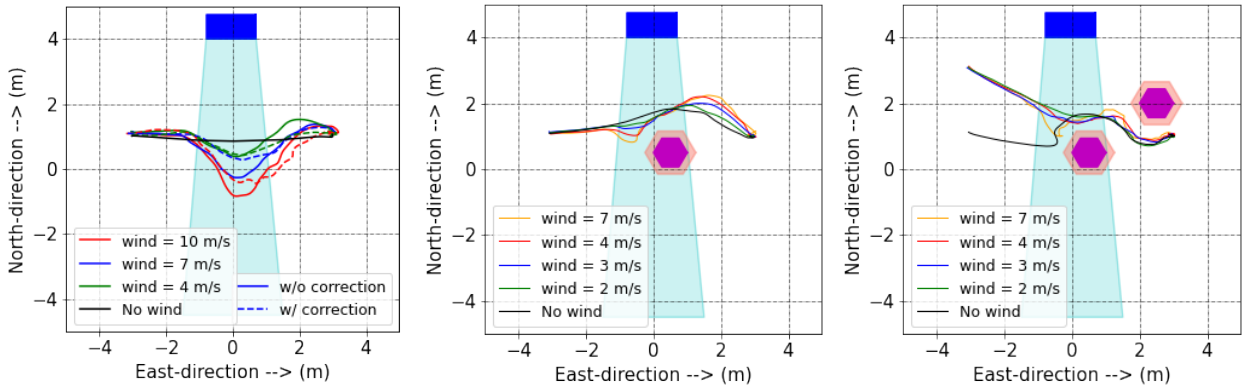
Fig. 5 Streamlines and paths of vehicles with different start positions and destinations.

Vehicles are assumed to be point objects in velocity calculations. On the other hand, real vehicles have a finite volume. In order to take the vehicle volume into account, obstacle boundaries are inflated by an amount equal to vehicle radius. Throughout the paper, solid magenta shapes represent the real obstacles and shaded areas are the obstacle boundaries obtained after inflation. In panel method calculations, these inflated obstacle boundaries are considered.

In Fig 5, streamlines and paths of two different vehicles are plotted together. The blue circle marks the vehicle start position and the green cross marks the vehicle goal position where a sink element is located. By definition, streamlines cannot enter into obstacles or cross each other. Consequently, vehicles following streamlines, can arrive at any desired destination point from any arbitrary starting position on the map with obstacle avoidance guarantee.

B. Indoor Tests with WindShape

To test the robustness of the algorithm under effects of unknown wind gusts the wind generator shown in Fig. 3 is used. *WindShape* is a modular wind generator located inside ENAC's indoor flight facility.

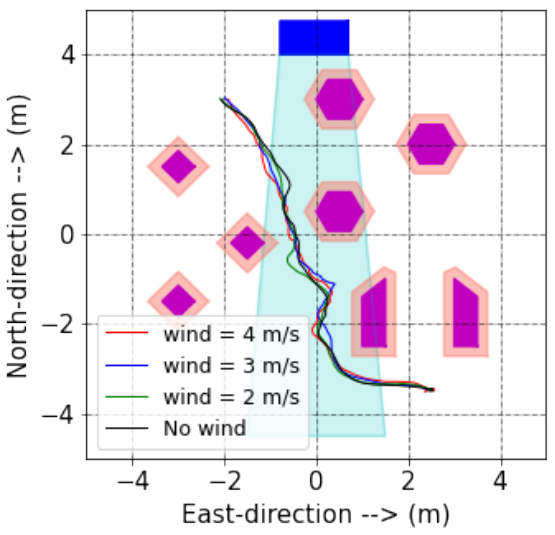


(a) Case 1: Empty arena. **(b) Case 2: Arena with one building.** **(c) Case 3: Arena with two buildings.**

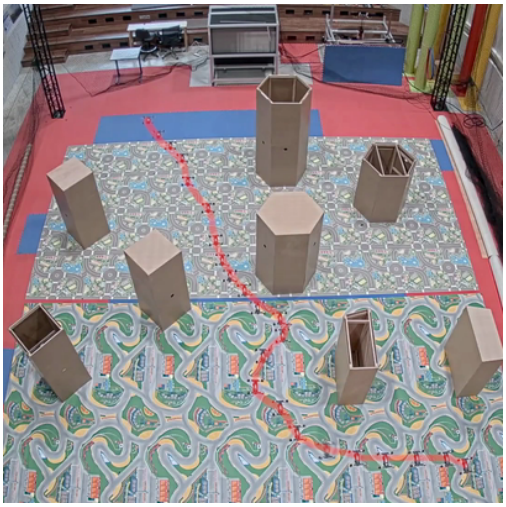
Fig. 6 Trajectories under wind disturbance.

To assess the effectiveness of panel method under wind disturbance three basic cases are considered and plotted

on Fig. 6. First, to compare the performance of panel method and wind correction term, both methods are tested in an empty arena under wind disturbance. Results are presented in Fig. 6a. Here, wind speed (measured at the exit of WindShape) is gradually increased from $0m/s$ to $10m/s$ and the vehicle is tasked with flying on a straight line. In Fig. 6a, solid lines are the trajectories obtained from panel method solution and dashed lines are trajectories generated by panel method with correction term. The improvement introduced by the correction term is evident in this plot. Especially at higher wind speeds correction term reduces the deviation from original path significantly. Therefore, for the rest of the experiments panel method with correction term is used for path planning.



(a) Trajectories for scenario 1.



(b) Images captured from experiment with wind speed, $V_w = 4m/s$ for scenario 1.

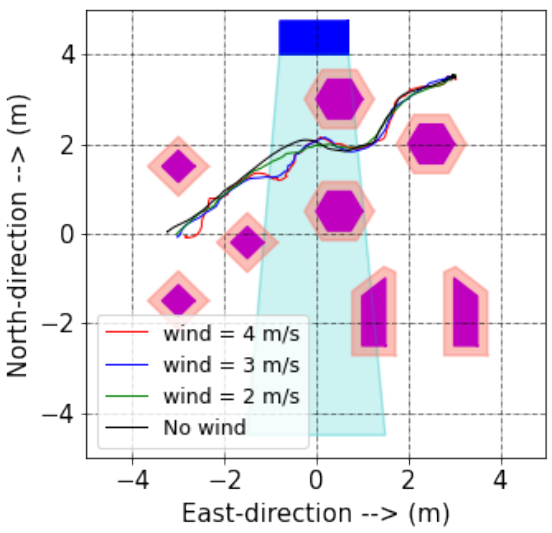
Fig. 7 Scenario 1: Travelling downstream in wind cone.

For the second case, a building is placed downstream of the wind to check whether the wind disturbance can cause a collision to an obstacle. As it can be observed from Fig. 6b, the vehicle avoids the building when the the wind speed is as high as $7m/s$. However, this time the vehicle overshoots as soon as it exits the WindShape cone. This sort of overshoot is expected since there is a sudden change in wind speed at the exit of wind generator cone and velocity correction only uses instantaneous velocity error as opposed to prediction of desired path multiple steps ahead. Hence, for the third case, an other building is placed at the overshooting position to check whether this overshoot movement would cause a collision. In Fig. 6c, trajectories for the third case are plotted. In this scenario, in order to force the vehicle between buildings starting position is shifted $1m$ towards north. In this case too, panel method prevents collision with both obstacles under wind gust.

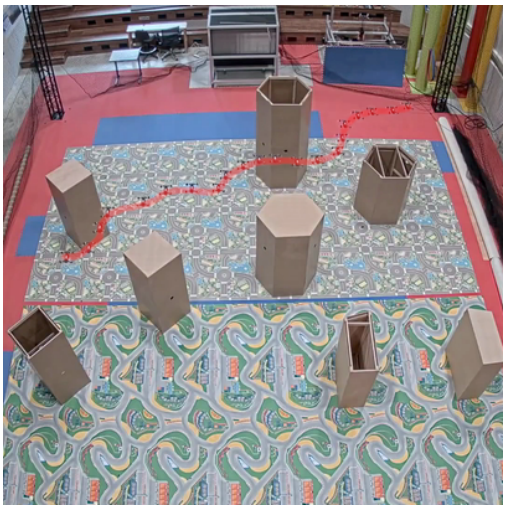
In Fig. 7, an example scenario for a single air taxi in an scaled urban environment is plotted. For this scenario the vehicle is tasked with picking up a passenger from its start position in north west and travel to its destination in south east. This mission requires the air taxi to travel downstream in wind cone generated by WindShape. In Fig. 7a, trajectory logs from experiments conducted at different wind speeds are plotted together. Although the disturbance caused by the wind is evident, the air taxi arrives to its destination without much deviation from the original path. In Fig. 7b, sequential image captures from the experiment with wind speed of $4m/s$ are presented.

Second example scenario where an air taxi is tasked with travelling from west to east is presented in Fig. 8. In this mission the air taxi has to travel across the wind cone generated by WindShape. In Fig. 8a, trajectory logs from experiments conducted at different wind speeds are plotted together. Especially at high wind speeds there is visible deviation from the original path. Nonetheless, the air taxi follows a collision free path and arrives to the desired destination. In Fig. 8b, sequential image captures from the experiment with wind speed of $4m/s$ are presented.

Multiple vehicles. For urban mobility applications, planning collision free paths for multiple vehicles is a necessity.

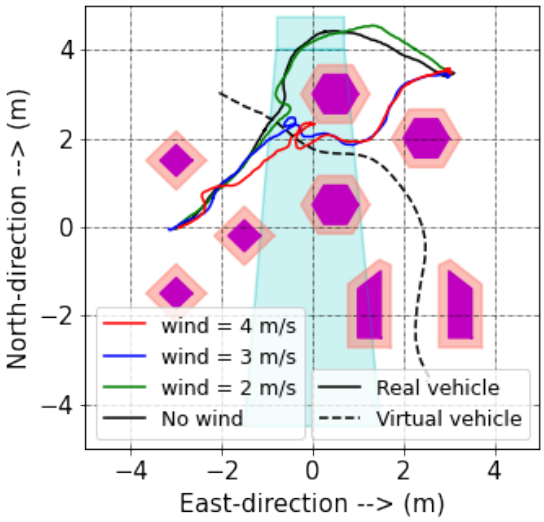


(a) Trajectories for scenario 2.

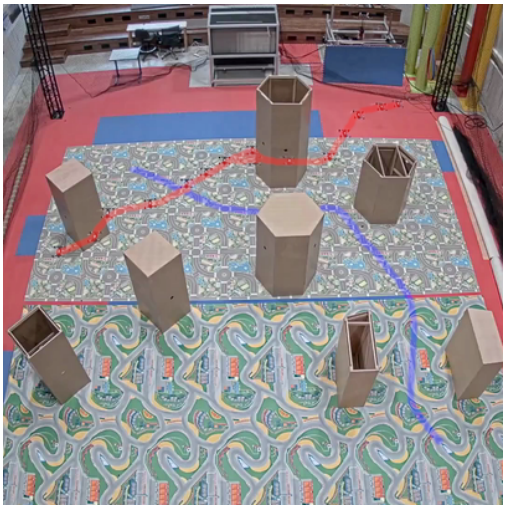


(b) Images captured from experiment with wind speed, $V_w = 4m/s$ for scenario 2.

Fig. 8 Scenario 2: Travelling across wind cone.



(a) Trajectories for scenario 3.

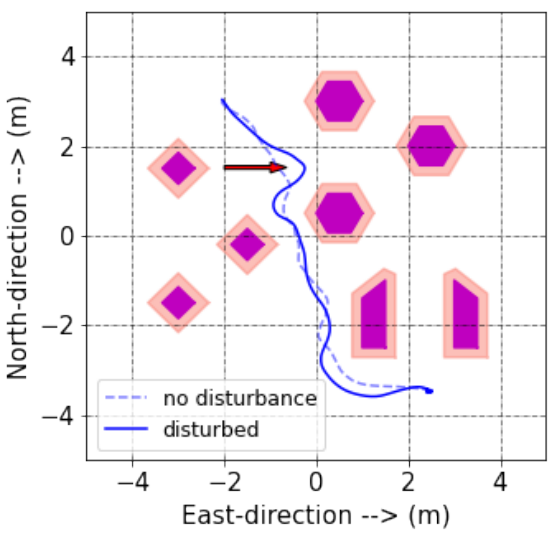


(b) Images captured from experiment with wind speed, $V_w = 4m/s$ for scenario 3.

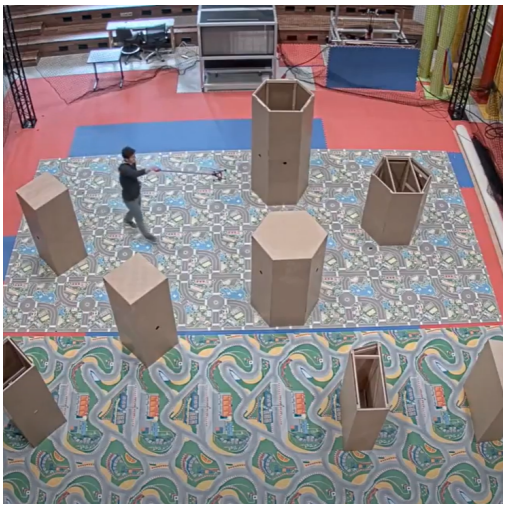
Fig. 9 Scenario 3: Path planning for real vehicle and virtual vehicle.

To that end, a virtual vehicle is included to the experiments throughout Paparazzi's dynamic simulation. Experiment with the virtual vehicle is presented in Fig. 9. Here, the mission of the virtual vehicle is to travel from north east to its goal in south west. Similarly, the real vehicle travels from west to east. Both vehicles are modelled as point source elements in calculations to prevent any collisions. Furthermore, this experiment is conducted under different wind speeds. In Fig. 9a, trajectory logs from experiments conducted at different wind speeds are plotted together. To avoid collision with the virtual vehicle, real vehicle follows a path around hexagonal buildings. However, when the wind speed is larger than $3m/s$, the real vehicle is forced to take the path between hexagonal buildings. In either case, there is no collision with the virtual vehicle. In Fig. 9b, sequential image captures from the experiment with wind speed of $4m/s$ are presented.

The last but not least, a final scenario for indoor arena is presented in Fig. 10. In this scenario a different type of disturbance is considered which is other than wind. The vehicle is tasked with travelling from north west to south east.



(a) Trajectory under sudden disturbance.



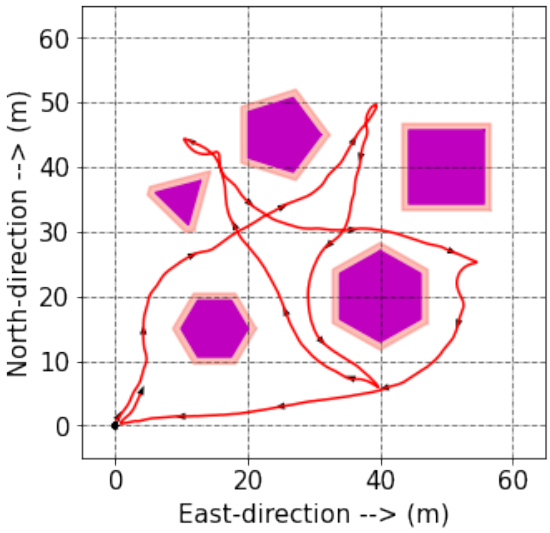
(b) Image captured from experiment with sudden disturbance.

Fig. 10 Scenario with sudden disturbance.

At the position indicated with the red arrow in Fig. 10a the quad-rotor is pushed towards east with a stick. Although this disturbance causes the vehicle to follow a different streamline, it neither causes any collision nor prevents the vehicle from reaching its goal.

C. Outdoor Tests

Outdoor experiments are conducted in a local RC airfield runway located in Muret, France, as shown in Fig. 4a. For the outdoor scenarios, there are no real buildings on the test area. Instead, no-fly zones with different shapes are



(a) Recorded trajectory for outdoor experiment.

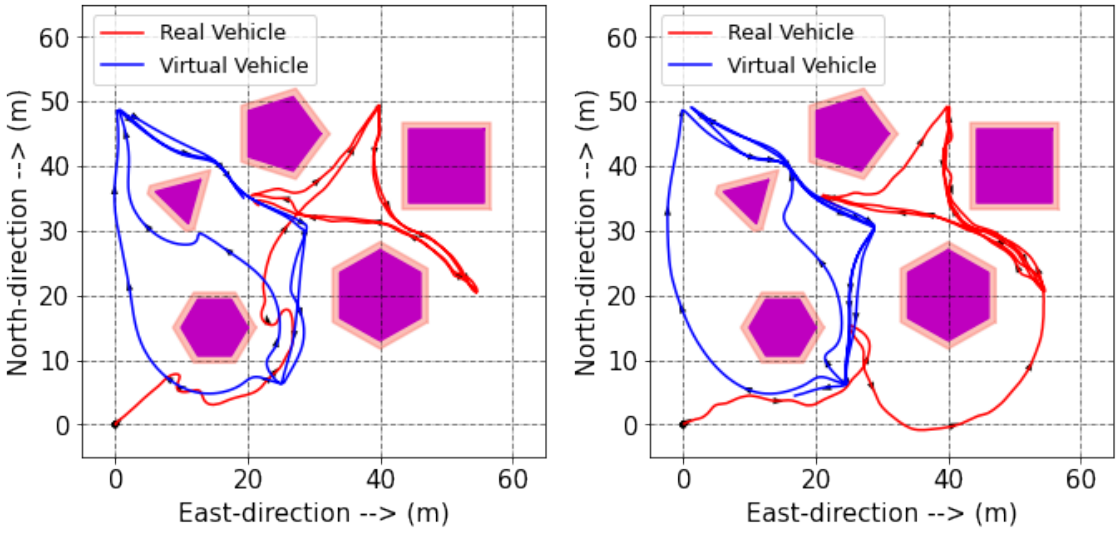


(b) Satellite image captured from experiment.

Fig. 11 Outdoor experiment with single vehicle.

defined on the outdoor arena. No-fly zones are marked with magenta colored polygons on the map as shown in Fig. 11b. Shaded areas are the safety perimeter around buildings. Safety perimeter for outdoor experiments were taken as $1m$ (as opposed to $20cm$ safety perimeter in indoor arena) due to greater sensor errors that had to be considered such as GPS

accuracy, heading information from magnetometer, etc...



(a) Trajectories of vehicles for $\sigma = 0.95$. **(b) Trajectories of vehicles for $\sigma = 1.5$.**

Fig. 12 Outdoor experiment with one real and one virtual vehicle.

In Fig. 11, outdoor experiment for a single vehicle is plotted. Similar to indoor tests, no-fly zones are also inflated as a safety precaution. Inflated boundaries are plotted with shaded pink color. For this scenario, the vehicle starts from origin and is tasked with traveling to four goal positions sequentially and returning to origin again. Trajectory of the vehicle is plotted in Fig. 11a and satellite image capture from the experiment is presented in Fig. 11b.

Multiple vehicles. In Fig. 12, outdoor experiments with one real and one virtual vehicle are presented. In this scenario, the real vehicle flies together with a virtual vehicle. Vehicles are tasked with travelling between 3 different goal positions sequentially while avoiding each other and no-fly zones. Both vehicles are modelled as point source elements in panel method calculations to prevent collisions. Source strength is a design parameter. In Fig. 12a, trajectories of an experiment with relatively low source strength is given. In this case, both vehicles enter narrow corridors between no-fly zones and do not alter their path until they get close enough to the other vehicle. For the second case plotted in Fig. 12b, same scenario is repeated with larger source strength. This time, instead of entering narrow passages between no-fly zones, vehicles take a detour around virtual obstacles and avoid each other completely.

VI. Conclusion

In this study, robustness of panel method based path planning is explored through hardware experiments both in indoor and outdoor test facilities. Potential field generated by panel method guarantees obstacle avoidance and global convergence [26]. This property, enables panel method based path planning algorithm to inherently overcome disturbances. Even if the vehicle deviates from its original path due to some disturbance, the new position still leads the vehicle to the global minima. In order to reduce the deviation from original path, a correction term is introduced and fed back to the velocity calculation with a PD controller. Furthermore, obstacle avoidance and goal convergence capabilities of the panel method based path planning algorithm under wind gust disturbances are evaluated through indoor and outdoor test campaigns.

Indoor experiments suggest that, panel method based algorithm is robust against wind gust disturbances. Even under effect of wind, vehicles can avoid obstacles and arrive desired goal positions. The velocity correction term improves disturbance rejection and decreases the deviation from original path.

Outdoor experiments were more challenging than indoor tests in the sense that not only there were wind disturbance but also greater sensor errors had to be considered such as GPS accuracy, heading information from magnetometer, etc...

For this reason, larger safety perimeters are defined around no-fly zones. Outdoor experiments are conducted in an open area with no buildings to disturb the wind flow. Effect of wind around real buildings could not be observed.

Current method neither has memory nor has any knowledge about future path. On the other hand, panel method requires little computational power and can generate longer path segments faster than controller feedback rate. Instead of instantaneous errors, feeding a longer segment of the original path can improve disturbance rejection property of the proposed method, which is going to be handled in our future work.
All in all, both indoor and outdoor flight tests suggests that panel method based path planning algorithm is a promising tool for path planning in urban airspace with decent disturbances rejection and guaranteed global convergence.

Acknowledgments

Authors would like to thank Cédric Boutet and Laurent Lacaze for the construction of scaled urban environment at ENAC and Xavier Paris for the indoor flight arena technical support and finally the open-source community of the Paparazzi Autopilot System. Through out this work Author Z. Bilgin was funded by Campus France.

References

[1] O'Hear, "Lilium, a German company building an electric 'air taxi', makes key hires from Gett, Airbus and Tesla." Retrieved 12 November, 2020, from. https:// techcrunch.com/2017/08/22/lilium/, 2017.

[2] Hawkins, "Hyundai will make flying cars for Uber's air taxi service." Retrieved 12 November 2020, from https://www.theverge.com/2020/1/6/21048373/hyundaiflying-car-uber-air-taxi-ces-2020, Jan. 2020.

[3] Jasper, C., "Air-Taxi Startup Volocopter Boosts Funds in Race to Get Flying." Retrieved 9 April 2021, from https://www.bloomberg.com/news/articles/2021-03-03/air-taxi-startup-volocopter-boosts-funds-in-race-to-get-flying, 2021.

[4] Reichmann, K., "Airbus Unveils New eVTOL Aircraft." Retrieved 18 October 2021, from https://www.aviationtoday.com/2021/09/22/airbus-unveils-new-evtol-aircraft/, Sep. 2021.

[5] Bauranov, A., and Rakas, J., "Designing airspace for urban air mobility: A review of concepts and approaches," *Progress in Aerospace Sciences*, Vol. 125, 2021, p. 100726. https://doi.org/https://doi.org/10.1016/j.paerosci.2021.100726, URL https://www.sciencedirect.com/science/article/pii/S0376042121000312.

[6] Teshnizi, M., Kosari, A., Goliaei, S., and Shakhesi, S., "Centralized Path Planning for Multi-aircraft in the Presence of Static and Moving Obstacles," *International Journal of Engineering*, Vol. 33, No. 5, ????

[7] Chen, Y., Luo, G., Mei, Y., Yu, J., and Su, X., "UAV path planning using artificial potential field method updated by optimal control theory," *International Journal of Systems Science*, 2014.

[8] Ge, D., and Topcu, U., "Hierarchical path planning for urban on-demand air mobility," *2019 IEEE Conference on Control Technology and Applications (CCTA)*, 2019.

[9] Pradeep, P., and Wei, P., "Energy-Efficient Arrival with RTA Constraint for Multirotor eVTOL in Urban Air Mobility," *Journal of Aerospace Information Systems*, Vol. 16, No. 7, ????

[10] Lifen, L., Ruoxin, S., Shuandao, L., and Jiang, W., "Path planning for UAVS Based on Improved Artificial Potential Field Method through Changing the Repulsive Potential Function," *Proceedings of 2016 IEEE Chinese Guidance, Navigation and Control Conference*, 2016.

[11] Yingkun, Z., "Flight path planning of agriculture UAV based on improved artificial potential field method," *2018 Chinese Control And Decision Conference (CCDC)*, 2018.

[12] Liu, Y., and Zhao, Y., "A Virtual-Waypoint Based Artificial Potential Field Method for UAV Path Planning," *Proceedings of 2016 IEEE Chinese Guidance, Navigation and Control Conference*, 2016.

[13] Wang, H., Lyu, W., Yao, P., Liang, X., and Liu, C., "Three-dimensional path planning for unmanned aerial vehicle based on interfered fluid dynamical system," *Chinese Journal of Aeronautics*, Vol. 28, No. 1, ????

[14] Li, W., Yang, C., Jiang, Y., Liu, X., and Su, C.-Y., "Motion Planning for Omnidirectional Wheeled Mobile Robot by Potential Field Method," *Journal of Advanced Transportation*, Vol. 2017, 2017, pp. 1–11. https://doi.org/10.1155/2017/4961383.

[15] Hosseini Rostami, S. M., Kumar, A., Wang, J., and Liu, X., "Obstacle avoidance of mobile robots using modified artificial potential field algorithm," *EURASIP Journal on Wireless Communications and Networking*, Vol. 2019, 2019. https://doi.org/10.1186/s13638-019-1396-2.

[16] Kim, J.-O., and Khosla, P., "Real-time obstacle avoidance using harmonic potential functions," *IEEE Transactions on Robotics and Automation*, Vol. 8, No. 3, 1992, pp. 338–349. https://doi.org/10.1109/70.143352.

[17] Masoud, A. A., "A harmonic potential field approach for joint planning and control of a rigid, separable nonholonomic, mobile robot," *Robotics and Autonomous Systems*, Vol. 61, No. 6, 2013, pp. 593–615. https://doi.org/https://doi.org/10.1016/j.robot.2013.02.007, URL https://www.sciencedirect.com/science/article/pii/S0921889013000432.

[18] Fahimi, F., *Autonomous robots*, Springer, 2010.

[19] Daily, R., and Bevly, D. M., "Harmonic potential field path planning for high speed vehicles," *2008 American Control Conference*, 2008, pp. 4609–4614. https://doi.org/10.1109/ACC.2008.4587222.

[20] Garrido, S., and Moreno, L., "Robotic Navigation using Harmonic Functions and Finite Elements." 2006, pp. 94–103.

[21] Liang, X., Wang, H., Li, D., and Liu, C., "Three-dimensional path planning for unmanned aerial vehicles based on fluid flow," *2014 IEEE Aerospace Conference*, 2014.

[22] Zhang, Y., and Valavanis, K. P., "A 3-D Potential Panel Method for Robot Motion Planning," *Robotica*, Vol. 15, No. 4, ????

[23] Uzol, O., Yavrucuk, I., and SezerUzol, N., "Panel-Method-Based Path Planning and Collaborative Target Tracking for Swarming Micro Air Vehicles," *Journal of Aircraft*, Vol. 47, No. 2, ????

[24] Velagić, J., Vuković, L., and Ibrahimović, B., "Mobile Robot Motion Framework Based on Enhanced Robust Panel Method," *International Journal of Control, Automation and Systems*, Vol. 18, No. 5, 2020, pp. 1264–1276.

[25] Unal, Z., and Yavrucuk, I., "Panel Method Based Path Planning for eVTOL in Urban Environment," *Vertical Flight Society Forum 77*, 2021.

[26] Bilgin, Z., Bronz, M., and Yavrucuk, I., "Experimental Evaluation of Panel-Method-Based Path Planning for eVTOL in A Scaled Urban Environment," *Vertical Flight Society Forum 78*, 2022.

[27] ENAC, "Drone Flight Arena Toulouse Occitanie," Ecole Nationale de l'Aviation Civile, Retrieved 19 October 2021, from https://www.enac.fr/en/drone-flight-arena-toulouse-occitanie-0, 2021.

[28] Anderson, J. D., *Fundamentals of Aerodynamics*, 5^{th} ed., McGraw-Hill, 2011.

[29] Katz, J., and Plotkin, A., *Low Speed Aerodynamics*, Cambridge Univ. Press, Cambridge, UK, 2001.

[30] Hattenberger, G., Bronz, M., and Gorraz, M., "Using the Paparazzi UAV System for Scientific Research," *International Micro Air Vehicles Conference and Flight Competition*, Delft, Netherlands, 2014, pp. 247–252. https://doi.org/10.4233/uuid:b38fbdb7-e6bd-440d-93be-f7dd1457be60.

[31] Smeur, E., de Croon, G., and Chu, Q., "Cascaded incremental nonlinear dynamic inversion for MAV disturbance rejection," *Control Engineering Practice*, Vol. 73, 2018, pp. 79–90. https://doi.org/https://doi.org/10.1016/j.conengprac.2018.01.003, URL https://www.sciencedirect.com/science/article/pii/S0967066118300030.